Computer Physics Communications 195 (2015) 14–22

Contents lists available at ScienceDirect

Computer Physics Communications

journal homepage: www.elsevier.com/locate/cpc

A discrete-element model for viscoelastic deformation and fracture of glacial ice

T.I. Riikilä [a,*], T. Tallinen [a], J. Åström [b], J. Timonen [a,c]

[a] University of Jyväskylä, Department of Physics and Nanoscience Center, P.O. Box 35 (YFL), FI-40014, Jyväskylä, Finland

[b] CSC - It-centre for science, P.O. Box 405, FIN-02101, Esbo, Finland

[c] ITMO University, Kronverkskii ave. 49, 197101, Saint Petersburg, Russia

ARTICLE INFO

Article history:
Received 21 October 2014
Received in revised form
9 April 2015
Accepted 13 April 2015
Available online 21 April 2015

Keywords:
DEM
Viscoelastic
Fragmentation
Ice

ABSTRACT

A discrete-element model was developed to study the behavior of viscoelastic materials that are allowed to fracture. Applicable to many materials, the main objective of this analysis was to develop a model specifically for ice dynamics. A realistic model of glacial ice must include elasticity, brittle fracture and slow viscous deformations. Here the model is described in detail and tested with several benchmark simulations. The model was used to simulate various ice-specific applications with resulting flow rates that were compatible with Glen's law, and produced under fragmentation fragment-size distributions that agreed with the known analytical and experimental results.

1. Introduction

In the last few decades computer efficiency has increased dramatically, paving the way for an increasing number of different applications of discrete-element methods (DEMs). DEM models have been used to investigate the behavior of a large variety of materials in many different fields of science. The huge amount of possibilities becomes evident in, e.g., Ref. [1]. To mention just a few: the evolution of shear zones in sand for earth-pressure problems [2], energy dissipation and particle motion in ball mills [3], oedometric tests for railway ballast [4], silo discharge of a cohesive solid [5], and the behavior of cohesive soil operated by bulldozer blades [6].

There are DEM models that include properties like elasticity, viscosity, and brittle behavior, but very rarely all of them. To investigate the behavior of ice (or a material of similar kind) in its full complexity, we need to incorporate all of the above properties so as to include the complex nonlinear rheology of ice. Some papers, where the aforementioned properties have been taken into consideration, can be found in, e.g., Ref. [7]. In that reference the material behavior was elasto-plastic, but plasticity was achieved in a time-dependent way, and the behavior could therefore be considered to be viscoelastic. There are also some models developed within the field of glaciology, which are specific to ice. A few models exist for the pure elastic behavior with fracture [8] and [9], and Ref. [10] describes a model, where individual ice elements can deform plastically, but cannot move relative to each other without permanent breakup. In this investigation a new DEM model for viscoelastic materials with fracture is introduced. It is important to realize that all the properties of the model do not necessarily appear simultaneously. Viscous behavior is present as long as the stresses in the material are below the fracture threshold. When this threshold is exceeded the material begins to fracture, and its brittle properties begin to dominate. Elasticity is always present as the basic property of the model. This model is described in detail, and results of benchmark simulations are compared to those of analytical and empirical considerations.

2. Model

The model consists of two-dimensional (2D) random-sized discs which are connected together with massless elastic beams. Formulation of the model begins with the elastic energy of a single beam,

$$E_{tot} = \frac{1}{2}k_s\epsilon^2 + \frac{1}{2}k_b(\theta_1^2 + \theta_2^2), \quad (1)$$

* Corresponding author.
E-mail addresses: timo.i.riikila@student.jyu.fi (T.I. Riikilä), tuomas.tallinen@jyu.fi (T. Tallinen), jan.astrom@csc.fi (J. Åström), jussi.t.timonen@jyu.fi (J. Timonen).

http://dx.doi.org/10.1016/j.cpc.2015.04.009
0010-4655/

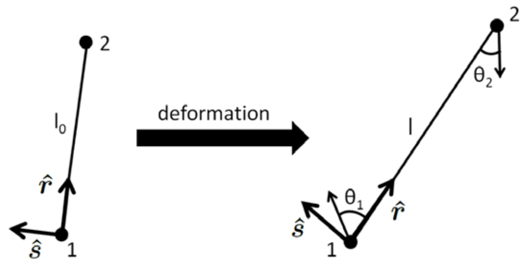

Fig. 1. A beam between particles 1 and 2 before and after deformation. $\hat{\boldsymbol{r}}$ is the unit vector in the direction of the beam connecting the two discs, and $\hat{\boldsymbol{s}}$ is the unit vector in the perpendicular direction. Beam's equilibrium length and length after deformation are denoted by l_0 and l, respectively. Angles θ_1 and θ_2 denote rotations with respect to the axis at both ends of the beam.

where ϵ, θ_1, and θ_2 are the axial strain and rotation angles of the two ends relative to the axis of the beam, respectively, and k_s and k_b are the corresponding stiffness parameters. The corresponding forces and torques acting on the two ends of the beam can be derived from the energy, Eq. (1), in the form

$$\begin{aligned} \boldsymbol{f}_1 &= \frac{k_s\epsilon}{l_0}\hat{\boldsymbol{r}} - \frac{k_b(\theta_1+\theta_2)}{l}\hat{\boldsymbol{s}}, \\ \boldsymbol{f}_2 &= -\frac{k_s\epsilon}{l_0}\hat{\boldsymbol{r}} + \frac{k_b(\theta_1+\theta_2)}{l}\hat{\boldsymbol{s}}, \\ \tau_1 &= k_b\theta_1, \\ \tau_2 &= k_b\theta_2, \end{aligned} \tag{2}$$

where l_0 and l are the equilibrium and deformed length of the beam, respectively. The axial unit vector, $\hat{\boldsymbol{r}}$, and the unit vector, $\hat{\boldsymbol{s}}$, perpendicular to the axis are shown in Fig. 1. Deformation of the beam in the axial direction is damped by forces

$$\boldsymbol{f}_1^{\mu} = s_{\mu}\dot{l}\hat{\boldsymbol{r}}, \qquad \boldsymbol{f}_2^{\mu} = -s_{\mu}\dot{l}\hat{\boldsymbol{r}}, \tag{3}$$

and an off-axis deformation is damped by torques

$$\tau_1^{\mu} = -b_{\mu}\dot{\theta}_1, \qquad \tau_2^{\mu} = -b_{\mu}\dot{\theta}_2, \tag{4}$$

where dots denote time derivatives. Coefficients s_{μ} and b_{μ} are selected so that deformation of the beam is underdamped. When two discs are not connected with a beam, the repulsive part of the beam energy is used as a contact potential to prevent their overlap. Collisions between discs are inelastic, with a velocity-dependent damping force similar to the axial damping force of a beam, in order to allow dissipation of energy. A beam breaks if it is deformed beyond a threshold limit, which can be chosen as a limiting maximum stress, strain, or elastic energy. Energy thresholds are used throughout this paper. In our viscoelastic simulations, a beam was also allowed to break below the fracture threshold with a probability that depended on the stress applied to it. When complemented by a rule to create new beams between discs that were close to each other, this allowed the material to undergo slow stress-dependent viscous flow. These fracture rules are detailed in the simulation sections below. Body forces used in the model were gravity and buoyancy, and others are easy to add. The Newtonian dynamics of the discs were simulated using an explicit scheme,

$$\begin{aligned} \boldsymbol{a}_i(t) &= \boldsymbol{F}^i_{tot}(t)/m_i \\ \boldsymbol{v}_i(t) &= \boldsymbol{v}_i(t-\Delta t) + \boldsymbol{a}_i(t)\Delta t \\ \boldsymbol{r}_i(t) &= \boldsymbol{r}_i(t-\Delta t) + \boldsymbol{v}_i(t)\Delta t \end{aligned} \tag{5}$$

$$\begin{aligned} \boldsymbol{\alpha}_i(t) &= \boldsymbol{\tau}_i(t)/I_i \\ \boldsymbol{\omega}_i(t) &= \boldsymbol{\omega}_i(t-\Delta t) + \boldsymbol{\alpha}_i(t)\Delta t \\ \boldsymbol{\theta}_i(t) &= \boldsymbol{\theta}_i(t-\Delta t) + \boldsymbol{\omega}_i(t)\Delta t, \end{aligned} \tag{6}$$

where Eqs. (5) and (6) correspond to translational and rotational degrees of freedom, respectively. In Eqs. (5), $m_i = \pi\rho r_i^2$ is the mass of disc i with material density ρ and radius r_i. In Eqs. (5), $\boldsymbol{F}^i_{tot}$ is the sum of all forces acting on disc i, and $\boldsymbol{a}_i$, $\boldsymbol{v}_i$, and $\boldsymbol{r}_i$ are the acceleration, velocity, and position of disc i, respectively. Similarly in Eqs. (6), the angular acceleration, angular velocity, and rotation angle of disc i are denoted by $\boldsymbol{\alpha}_i$, $\boldsymbol{\omega}_i$, and $\boldsymbol{\theta}_i$, respectively. The total torque acting on disc i is $\boldsymbol{\tau}_i$, and $I_i = \pi\rho/2r_i^4$ is its moment of inertia. Time step Δt can be scaled as $\Delta t \sim \sqrt{\rho r/Y}$, where Y is Young's modulus of the material (see below). Typical values for the time step used in our simulations were 10^{-5}–10^{-4} s. A flow chart presenting the basic structure of the model is shown in Fig. 2.

2.1. Formation of the simulation lattice

A simulation lattice was generated by selecting a given number of random-sized discs from a chosen diameter distribution, and placing them loosely on a column above the floor of a rigid-wall container. Gravity was then applied to the discs, which caused them to fall and pile up on top of each other inside the container as shown in Fig. 3. A polydisperse collection of discs has the advantage over a monodisperse collection in that equal-sized discs inevitably form a regular lattice which is not isotropic, and, therefore, not ideal for simulating the physical fracture of isotropic materials. In Fig. 3 discs of diameters of 0.5–2.0 m were used to fill a container of the size 45 m × 45 m. The only interaction force between discs in the simulation shown in Fig. 3 was the repulsive contact force that kept the discs from overlapping. A similar overlap-dependent contact force was also used for the interaction between discs, and the walls of the container. After the lattice generation, Delaunay triangulation [11] was used to form candidates for the contact beams between discs. A connection suggested by Delaunay triangulation was accepted as a contact beam if it connected discs that were close enough to each other. This acceptance condition can be expressed in the form

$$d \le C(r_1 + r_2), \tag{7}$$

where d is the distance between discs, C is a constant larger than unity, and r_1 and r_2 are radii of discs that are candidates to be connected. If $C = 1$, the coordination number of the lattice would be low resulting in a too weakly connected material. However, C cannot be very large ($C \le 2$) because Delaunay triangulation typically creates very long connections at the edges of the lattice, and if C is too large, a beam can be formed between two discs with an unconnected disc in between them (see Fig. 4).

2.2. Elastic moduli

Owing to the random sizes and arrangement of the discs, elastic properties of the model are heterogeneous in a scale comparable to the disc size. In larger scales, however, simulation parameters k_s and k_b that control the stiffness of the beams, can be related to Young's modulus and Poisson's ratio of the material. Details of this derivation are shown in Appendix, and the total strain-energy density of the deformed lattice is given by (assuming a unit depth in the 2D system)

$$\begin{aligned} F &= \rho_b\left(\frac{k_s}{8} + \frac{k_b}{4}\right)(\epsilon_x^2 + \epsilon_y^2) \\ &\quad + \rho_b\left(\frac{k_s}{16} - \frac{k_b}{8}\right)(\epsilon_x^2 + 2\epsilon_x\epsilon_y + \epsilon_y^2), \end{aligned} \tag{8}$$

where ϵ_x and ϵ_y are strains in the x and y directions, respectively. Beam density, $\rho_b = c_C/r^2$, is the number of beams per unit area. Here c_C depends on the beam-length parameter, C, of Eq. (7), and r